HHS Public Access

Author manuscript

Dev Biol. Author manuscript; available in PMC 2024 May 01.

Published in final edited form as:

Dev Biol. 2024 May ; 509: 1–10. doi:10.1016/j.ydbio.2024.01.012.

Nkx2.3 transcription factor is a key regulator of mucous cell identity in salivary glands

Xin Gao[a,*], **Taro Mukaibo**[a,d,*], **Xiaolu Wei**[b], **Roberta C. Faustoferri**[b], **Maria S. Oei**[a], **Seo-Kyoung Hwang**[b,e], **Adela Jingyi Yan**[b], **James E. Melvin**[a,¶], **Catherine E. Ovitt**[b,c,¶]

[a]Secretory Mechanisms and Dysfunctions Section, National Institutes of Health, Bethesda, MD 20892, USA

[b]Center for Oral Biology, University of Rochester School of Medicine and Dentistry, Rochester, NY, 14642 USA

[c]Department of Biomedical Genetics, University of Rochester School of Medicine and Dentistry, Rochester, NY, 14642 USA

[d]Present address: Division of Oral Reconstruction and Rehabilitation, Kyushu Dental University, Kitakyushu, Fukuoka, Japan

[e]Present address: Pfizer Inc., Eastern Point Road, Groton, CT, 06340 USA

Abstract

Saliva is vital to oral health, fulfilling multiple functions in the oral cavity. Three pairs of major salivary glands and hundreds of minor salivary glands contribute to saliva production. The secretory acinar cells within these glands include two distinct populations. Serous acinar cells secrete a watery saliva containing enzymes, while mucous acinar cells secrete a more viscous fluid containing highly glycosylated mucins. Despite their shared developmental origins, the parotid gland (PG) is comprised of only serous acinar cells, while the sublingual gland (SLG) contains predominantly mucous acinar cells. The instructive signals that govern the identity of serous versus mucous acinar cell phenotypes are not yet known. The homeobox transcription factor Nkx2.3 is uniquely expressed in the SLG. Disruption of the *Nkx2.3* gene was reported to delay the maturation of SLG mucous acinar cells. To examine whether Nkx2.3 plays a role in directing the mucous cell phenotype, we analyzed SLG from *Nkx2.3*$^{-/-}$ mice using RNAseq, immunostaining and proteomic analysis of saliva. Our results indicate that Nkx2.3, most likely in concert with

¶Corresponding authors.
*Contributed equally

Author contributions

CEO and JEM designed the research.
TM, MSO, XW, SKH and AJY performed experiments and collected data.
XG, XW, MSO, TM, RCF, JEM and CEO analyzed data.
XG, RCF, XW, JEM and CEO wrote the manuscript.

The authors declare no competing financial or non-financial interests.

other transcription factors uniquely expressed in the SLG, is a key regulator of the molecular program that specifies the identity of mucous acinar cells.

Graphical Abstract

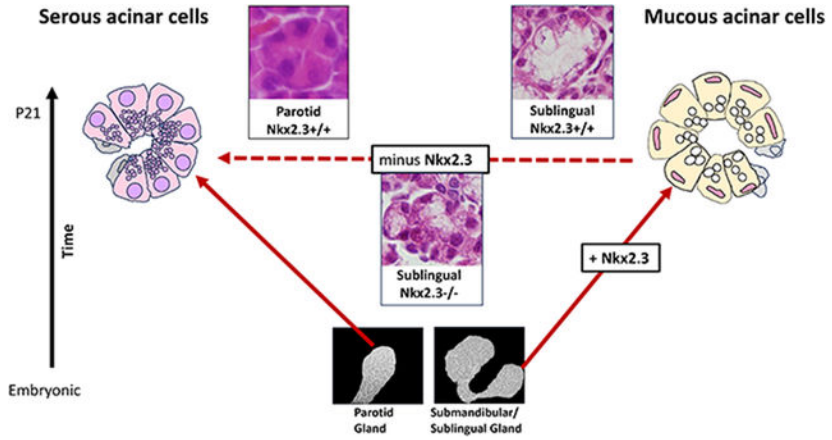

Keywords

sublingual salivary gland; acinar cells; mucous cell; Nkx2.3; transcription factor

Introduction

Saliva is produced by three pairs of major salivary glands and hundreds of minor salivary glands. The sublingual (SLG), submandibular (SMG) and parotid (PG) glands are each made up of clustered secretory acinar cells that drain saliva into a branching ductal system. Although they share developmental origins [(Rothova et al., 2012)] the glands differ in cellular makeup and consequently in the composition of saliva secreted by each. Serous acini in the PG secrete a watery fluid rich in enzymes, such as amylase, while mucous acini in the SLG produce a viscous secretion containing high molecular weight glycoproteins. These secretions combine to yield the total saliva which fulfills multiple functions in the oral cavity, including swallowing, speaking, host defense, tooth mineralization, wound healing and pH balance. Despite extensive study of salivary gland development [(Miletich, 2010; Patel and Hoffman, 2014)] little is known about the instructional signals that distinguish serous and mucous acinar cells.

Several transcription factors involved in cell fate determination have been characterized in the developing salivary glands [(Athwal et al., 2019) (Chatzeli et al., 2017) (Yoshida et al., 2001)]. However, RNA profiling of the major salivary glands in mice revealed that a limited number of transcription factors are differentially expressed in a manner specific to each of the three glands [(Gao et al., 2018)]. These data revealed 19 transcription factors, including Nkx2.3, that are uniquely expressed in the SLG.

Nkx2.3 belongs to a family of homeodomain genes known to play critical roles in cell type specification in many tissues [(Kim and Nirenberg, 1989) (Harvey, 1996) (Stanfel et al.,

2005)]. During embryonic development in mouse, *Nkx2.3* is expressed in oral and branchial arch ectoderm, as well as in spleen, midgut and hindgut [(Pabst et al., 1997)]. Deficiency of *Nkx2.3* alters normal developmental patterning and differentiation of several peripheral lymphoid organs, including the spleen and intestine [(Pabst et al., 1999)].

Within mouse and human salivary glands, the *Nkx2.3* gene is uniquely expressed in the SLG [(Biben et al., 2002) (Gao et al., 2018) (Saitou et al., 2020)]. Knockout of the murine *Nkx2.3* gene was reported to delay cell maturation in the SLG, suggesting a role for Nkx2.3 in specifying the mucous cell phenotype [(Biben et al., 2002)]. In this study, we analyzed the $Nkx2.3^{lacZ\Delta HD}$ mutant mouse strain [(Wang et al., 2000)] using immunohistochemistry, RNA-Seq and proteomic analysis of saliva to investigate whether Nkx2.3 is involved in directing the identity of mucous acinar cells.

Results

Disruption of SLG mucous cell phenotype in *Nkx2*.3 knockout mice

We used a previously published $Nkx2.3^{lacZ\Delta HD}$ knock-in mouse model [(Wang et al., 2000)], in which the homeodomain and conserved NK2-specific domains encoded by exon 2 of the *Nkx2.3* gene were replaced with an internal ribosome entry site linked to a nuclear beta-galactosidase (nLacZ) gene expression cassette and polyadenylation site (Fig. 1A). nLacZ reporter gene expression mirrors the endogenous expression of Nkx2.3 transcription factor in the SLG, as detected using in situ hybridization [(Biben et al., 2002; Wang et al., 2000)]. Consistent with the previous report [(Wang et al., 2000)], we detected nLacZ staining in embryonic SLG as early as embryonic day 15.5 (E15.5) (data not shown). Consistent with the exclusive expression of Nkx2.3 in the SLG, nLacZ staining was not detected in the SMG (Fig. 1B). Starting at E18.5, most proacinar cells, as well as some duct cells, expressed nLacZ in heterozygotes (Fig. 1B, D, F) and persisted in the adult SLG.

$Nkx2.3^{lacZ\Delta HD/+}$ heterozygotes (*Nkx2.3+/−*) were mated to generate $Nkx2.3^{lacZ\Delta HD/lacZ\Delta HD}$ (*Nkx2.3−/−*) mice. In earlier studies, postnatal lethality of more than half of *Nkx2.3−/−* pups was noted due to disrupted development of the spleen and small intestine [(Pabst et al., 1999) (Wang et al., 2000)]. In our study, 91 of 108 *Nkx2.3−/−* mice genotyped after day 7 survived to adulthood. However, inclusion of dead pups found within 24 hours of birth lowered the survival rate of *Nkx2.3−/−* mice to 72%. The body weight of surviving *Nkx2.3−/−* mice is not significantly different from wild type or heterozygous littermates (Fig. S1A). However, both the weight and size of the SLG are reduced in *Nkx2.3−/−* compared to *Nkx2.3+/−* mice (Fig. S1B-D).

By E18.5, proacinar cells in the SLG are organized into secretory units [(Redman and Ball, 1978)]. Cytodifferentiation to mucous-secreting cells is reported to take place just before birth [(Denny et al., 1997)] and to continue during the postnatal period from P0 through P28 [(Das et al., 2009)]. Based on this developmental timeline, we analyzed SLG from *Nkx2.3+/−* and *Nkx2.3−/−* at three time points: E18.5, postnatal day 5 (P5) and postnatal day 21 (P21). In comparison to the heterozygotes, the number of nLacZ-stained nuclei in the *Nkx2.3−/−* SLG is lower, and the acini appear more compact and disorganized (Fig. 1C,E,G). H&E staining of paraffin sections also highlights the disorganized acini in the

Nkx2.3−/− SLG compared to the SLG in heterozygotes (Fig. S1E-H). Alcian blue was used to stain for mucous secretory cells producing acidic mucopolysaccharides. At E18.5 stained paraffin sections from *Nkx2.3−/−* SLG showed fewer mucopolysaccharide-producing cells in comparison to *Nkx2.3+/−* SLG (Fig. 2A,B). At postnatal timepoints P5 and P21, the number and size of Alcian blue-stained acini were lower in the *Nkx2.3−/−* SLG (Fig. 2C-F). These observations support the suggestion that mucous cell differentiation appears disrupted in *Nkx2.3−/−* SLG [(Biben et al., 2002)].

Gland-specific saliva was collected *ex vivo* from SLG after perfusion with cholinergic and beta-adrenergic agonists. Stimulated saliva secretion measurements showed a decrease in both the flow rate and total amount of saliva secreted from the SLG of *Nkx2.3−/−* compared to *Nkx2.3+/+* mice (Fig. 2G,H).

Nkx2.3−/− SLG express an intermediate transcriptome

We investigated the role of the Nkx2.3 transcription factor in specification of the mucous acinar cell phenotype by performing RNA-Seq on SLGs isolated from *Nkx2.3−/−* female mice (aged 8 and 33 weeks, n=4 each group). *Nkx2.3* gene expression in *Nkx2.3−/−* (SLG_{KO}) was compared with the previously published expression in wild type SLG (SLG_{WT}) after batch correction against house-keeping genes [(Li et al., 2017)]. As expected, *Nkx2.3* transcripts were decreased more than 5-fold (from 3.95 transcripts per million (TPM) to 0.85 TPM), in the SLG_{KO} compared to the wild type female SLG_{WT} (Fig. 3A).

In our earlier study, whole RNA-Seq was used to perform a simultaneous and unbiased evaluation of the expression levels of 14,300 genes in the three major salivary glands of mouse and revealed that each gland shows a unique transcriptional profile [(Gao et al., 2018)]. We employed principal component analysis (PCA) of the data combined with data from the previous study to determine whether the loss of Nkx2.3 altered the gene expression profile of the SLG. The transcriptional profile of the SLG_{KO} mapped with intermediate relatedness to the SLG_{WT} and wild type parotid gland (PG_{WT}) data, based on the batch-corrected whole transcriptomic outputs of all the 10 samples from the 3 gland types (Fig. 3B). The first two principal components accounted for a total of 86% (PC1:80% and PC2:6%) of data variation. This plot led us to speculate that loss of *Nkx2.3* expression in the SLG_{KO} results in a shift of gene expression in the SLG_{KO} toward the transcriptional profile of the PG_{WT}.

Comparison of transcriptomes in SLG_{KO}, SLG_{WT} and PG_{WT}

Comparison of the SLG_{WT} and SLG_{KO} transcriptomes revealed 496 significantly differentially expressed (DE) genes identified by the DESeq2 analysis (with adjusted P value <0.05). Altogether, 262 genes were down-regulated in the SLG_{KO} (Supplemental Table 1A) while 234 genes were up-regulated in the SLG_{KO} (Supplemental Table 1B) in comparison to the SLG_{WT}.

The intermediate profile observed in Fig. 3B suggests that loss of Nkx2.3 alters the SLG_{KO} transcriptome toward that of the PG_{WT}, the major salivary gland comprised of serous acinar cells. To determine if acinar fate decisions are still made in the SLG_{KO}, we examined expression of common acinar cell markers. The acinar cell-specific transcription factor

Mist1 (basic helix-loop-helix a15, Bhlha15) showed elevated expression in DESeq2 analysis of the SLG_{KO}, although this was not statistically significant (Fig. S2A). Using antibody staining, the water channel aquaporin 5 (AQP5) was detected in SLG of both *Nkx2.3+/−* and *Nkx2.3−/−* mice (Fig. S2B,C).

Heat maps were generated to compare the significantly DE gene expression profiles in SLG_{KO} with SLG_{WT} and with PG_{WT} (PG_{WT} data from [(Gao et al., 2018)]) (Fig. 4). Heat mapping of the top 80 down-regulated genes in the SLG_{KO} yielded an expression profile that resembles that of the PG_{WT} (Fig. 4A). Of the 262 significantly down-regulated genes in the SLG_{KO}, 109 genes (42%, highlighted in yellow, Table S1A) were decreased in both the SLG_{KO} and the PG_{WT} in comparison to expression in the SLG_{WT} (PG_{WT} data from [(Gao et al., 2018)]). We conclude that Nkx2.3 is a key transcriptional activator in the SLG_{WT}.

However, the loss of Nkx2.3 transcriptional activity also resulted in the up-regulation of 234 genes in the SLG_{KO} compared to expression in the SLG_{WT}. Although 48% (112 genes highlighted in yellow, Table S1B) of the genes up-regulated in the SLG_{KO} are genes more highly expressed in the PG_{WT} (PG_{WT} data from [(Gao et al., 2018)]), the heat map of the top 80 up-regulated genes does not mirror gene expression profiles of the PG_{WT} (Fig. 4B). In fact, many genes are up-regulated in the SLG_{KO} above levels found in either the SLG_{WT} or the PG_{WT} (Supplementary Table 1B; Fig. 4B,G).

Due to abnormal development of the spleen and disruption of leukocyte homing in surviving *Nkx2.3−/−* adult mice, we suspect that up-regulation of many genes in the SLG_{KO} may result from systemic activation of immune response pathways. The up-regulation of five secretoglobin genes, which encode small secreted proteins involved in immunoregulatory processes [(Mootz et al., 2022)], supports this conclusion (Fig. 4B). The up-regulation of the secreted protein prolactin-induced protein (Pip) is consistent with a shift in the transcriptome toward the PG_{WT}, as Pip expression is 20-fold higher in PG_{WT} compared to the SLG_{WT} (Fig. 4B). However, Pip expression is induced by cytokines and Pip is known to be involved in immunomodulatory functions [(Urbaniak et al., 2018)]. We conclude that Pip is most likely up-regulated due to the dysregulated immune activity in *Nkx2.3−/−* mice.

Down-regulation of genes associated with mucous cell function

To better understand the link between Nkx2.3 transcriptional activity and mucous acinar cells, we examined which genes exhibited altered expression. The GO terms for the DE up-regulated genes in the SLG_{KO} included protein metabolism and developmental processes. GO terms associated with DE down-regulated genes in the SLG_{KO} were cell organization & biogenesis, developmental processes, and signal transduction. Down-regulated genes encoded proteins central to mucous acinar cell functions, including secreted proteases, membrane channel proteins and proteins involved in glycosylation. Grouping the DE genes by function yielded heat maps that show the expression level of many genes in SLG_{KO} appears intermediate between that in the SLG_{WT} and the PG_{WT} (Fig. 4C-F).

Many genes down-regulated in the SLG_{KO} encode secreted proteins that are highly expressed in the SLG_{WT} (Fig. 4C). Several, such as Neurexophilin and PC-esterase protein (*Nxpe4*) and Brevican (*Bcan*) are found associated with extracellular matrix and may

function as scaffold proteins [(Xu et al., 2003)]. Absence of the Nkx2.3 transcription factor leads to reduced expression of many secreted proteins with potential immune functions. Glycoprotein 2 (*Gp2*), a pancreatic secretory glycoprotein, and surfactant protein D (*Sftpd*), expressed by alveolar cells in the lung, are linked to the innate immune response. Several C-C motif chemokine factors (*Ccl2, Ccl6, Ccl7, Ccl11* and *Ccl12*), which are chemotactic for macrophages during inflammation, were also down-regulated, as well as thrombospondin (*Thbs1*) and fibromodulin (*Fmod*) which are involved in cell-cell and cell-matrix interactions. In addition, 8 members of the serine protease kallikrein-related protein (*Klk1b*) gene family were significantly down-regulated in the SLG_{KO}. Kallikrein proteins are normally 10- to 100-fold more highly expressed in the SLG_{WT} than in the PG_{WT} [(Gao et al., 2018)], but the expression level of these down-regulated kallikrein genes in the SLG_{KO} is comparable to that found in serous cells of the PG_{WT} (Fig. 4D). Several genes encoding membrane channels are highly expressed in the SLG_{WT} but reduced in the PG_{WT} (Fig. 4E). In the SLG_{KO}, these genes were down-regulated compared to the SLG_{WT}, resulting in expression levels similar to those in the PG_{WT}.

Mucous acinar cells synthesize and post-translationally process highly-glycosylated proteins. A search for gene products associated with the synthesis or processing of glycoproteins revealed 8 genes that were significantly down-regulated in the SLG_{KO} compared to the SLG_{WT} (Fig. 4F). Staining with Alcian blue showed that mucin polysaccharides are produced by some cells of the SLG_{KO} (Fig. 2). We postulate that reduced or altered expression of glycosylation-related genes in the SLG_{KO} may lead to disruption of protein processing pathways in mucous acinar cells of the *Nkx2.3−/−* mice.

Proteomic analysis of saliva from *Nkx2.3−/−* SLG confirms transcriptional changes

Based on the transcriptomic changes, as well as potential disruptions in protein processing, we performed a pilot proteomic analysis to investigate whether loss of Nkx2.3 leads to changes in saliva composition. Saliva samples collected *ex vivo* from *Nkx2.3+/+* and *Nkx2.3−/−* SLG of adult mice were analyzed using LC-MS/MS to examine differences in protein composition. Primary proteomic results are provided in Supplemental Table 2.

Using UniProt (https://www.uniprot.org/) protein designations, we searched the proteomics results for the cognate genes that were DE in the RNA-Seq analysis. Over 60 genes that were DE in the SLG_{KO} compared to the SLG_{WT} were found to have altered protein abundance between the *Nkx2.3−/−* and *Nkx2.3+/+* saliva samples (Table S3). Many showed a positive correlation of increased mRNA and protein expression in the absence of Nkx2.3. Several of the secretoglobin genes found to be significantly up-regulated in RNA analysis of the SLG_{KO} (Table S3) were also detected at higher abundance in saliva from *Nkx2.3−/−* mice compared to *Nkx2.3+/+* (Fig. S3). Three proteins highly expressed in serous cells, Pip, Agt and Aqp5, showed up-regulated mRNA expression and increased protein abundance in saliva collected from *Nkx2.3−/−* SLG in comparison to *Nkx2.3+/+* SLG (Table S3). However, positive correlation between increased expression level and protein abundance was not consistently observed. For example, RNA-Seq data showed a significant up-regulation of transcripts for Dtnb in SLG_{KO} similar to expression levels in the PG_{WT} (Table S3), but Dtnb protein was markedly less abundant in saliva of *Nkx2.3−/−* compared to *Nkx2.3+/+* SLG

(Fig. S3). Furthermore, RNA-Seq data showed down-regulation of mRNA from 8 kallikrein genes in the SLG_{KO}, but increased levels of secreted kallikrein proteins were detected in saliva from *Nkx2.3−/−* SLG (Table S3; Fig. S3). While loss of the Nkx2.3 transcription factor leads to a shift in gene and protein expression in mucous cells of the *Nkx2.3−/−* SLG, the combined RNA-Seq and proteomic data suggest a more complex effect, which may be due to the activity of additional transcription factors involved in directing mucous cell identity.

Aberrant expression of alternatively spliced Smgc/Muc19 mRNA and proteins in *Nkx2.3−/−* SLG

Mucin 19 (Muc19) and the Submandibular gland protein C (SmgC) are derived from a single gene through alternative splicing (Fig. S4A) [(Culp et al., 2004) (Zinzen et al., 2004)]. SmgC is expressed in the developing SLG and decreases postnatally while Muc19 expression is low during embryogenesis, increasing in abundance after birth [(Das et al., 2009) (Das et al., 2010)]. Postnatal differentiation of SLG mucous acinar cells was hypothesized to direct the switch between the alternatively spliced transcripts encoding SmgC and Muc19 [(Das et al., 2009)]. As knockout of *Nkx2.3* disrupts maturation of mucous acinar cells [(Biben et al., 2002)], we investigated this switch using qPCR and immunohistochemistry with antibodies to SmgC and Muc19 proteins. Sections of SLG isolated at E18.5 showed little difference in SmgC staining between *Nkx2.3+/−* and *Nkx2.3−/−* SLG (Fig. S4B,C). However, staining at P0 suggested higher SmgC protein abundance in the *Nkx2.3−/−* SLG compared to *Nkx2.3+/−* SLG (Fig. 5A,B), which remained higher in sections isolated at P21 (Fig. S4D,E). In contrast, stained sections revealed less Muc19 protein at P0 in the *Nkx2.3−/−* SLG relative to the *Nkx2.3+/−* SLG (Fig. 5C,D). These results suggest that alternative splicing of the transcripts encoding SmgC and Muc19 is disrupted during postnatal development in mucous cells of *Nkx2.3−/−* SLG. This is supported by qPCR analysis at P21, which shows higher SmgC mRNA expression and lower Muc19 mRNA expression in the SLG_{KO} compared to SLG_{WT} (Fig. 5E,F). However, by 33 weeks of age, this was reversed and transcripts for both SmgC and Muc19 were significantly higher in SLG_{KO} compared to SLG_{WT} (Fig. 5G,H). In addition, both proteins were detected at higher abundance in saliva collected from *Nkx2.3−/−* SLG at 12 to 16 weeks (Fig. S3). The reason for this discrepancy is not known. Neither SmgC nor Muc19 is included in the list of up-regulated DE genes (Table S1A,B, Table S3). We speculate that any delay in mucous cell maturation is overcome in adults but that effects due to loss of Nkx2.3 transcriptional activity, such as increased expression of secretory proteins or disruptions in protein processing, alter Muc19 and SmgC mRNA and protein levels.

Discussion

The instructive signals that distinguish serous and mucous acinar cell types remain unknown. A previous study revealed a unique transcriptional profile within each of the three major salivary glands in mice [(Gao et al., 2018)]. In the SLG, which is comprised predominantly of mucous acinar cells, we found 19 uniquely expressed transcription factors, including the homeodomain-containing factor Nkx2.3 [(Gao et al., 2018)]. In this study, we have demonstrated that the Nkx2.3 transcription factor plays a regulatory role in maintaining

the distinct identity of mucous cells in the SLG, and that loss of Nkx2.3 alters mucous cell identity toward the serous acinar phenotype.

Loss of the Nkx2.3 transcription factor was previously reported to disrupt mucous cell differentiation in the SLG [(Biben et al., 2002)]. To investigate the link between Nkx2.3 and the mucous cell phenotype, we utilized the *Nkx2.3*$^{lacZ\Delta HD}$ strain, in which an expression cassette encoding nuclear beta-galactosidase (nLacZ) was inserted into the second exon of the *Nkx2.3* gene, disrupting the coding sequence [(Wang et al., 2000)]. nLacZ staining patterns are identical in *Nkx2.3*$^{lacZ\Delta HD/+}$ and *Nkx2.3*$^{lacZ\Delta HD/lacZ\Delta HD}$ (−/−) SLG, indicating that the transcription factor is not required for specification of the SLG, or for viability of the cells.

Murine SLG development is initiated at ~E12.5 [(Miletich, 2010)], but proacinar cells in the SLG differentiate to mucous-secreting cells just before birth [(Redman and Ball, 1978)]. Extensive cytodifferentiation is reported to take place in the SLG during the postnatal period from P0 through P28 [(Das et al., 2009)]. Loss of *Nkx2.3* resulted in smaller, less organized acinar cells and an apparent reduction in mucous cell number in the SLG_{KO}. This was consistent with reduced cell proliferation noted in the small intestine of *Nkx2.3−/−* mutants [(Pabst et al., 1999)]. Despite the disorganized morphology, Alcian blue staining showed that acinar cells in the SLG_{KO} produce mucins, as previously reported [(Biben et al., 2002)]. nLacZ staining revealed that Nkx2.3 is also expressed in some duct cells, but morphological changes due to lack of Nkx2.3 in the ducts were not apparent.

Members of the Nkx2 transcription factor gene family are pivotal regulators of cell type specification in many tissues [(Desai et al., 2008; Sussel et al., 1998) (Wang et al., 2009) (Targoff et al., 2013; Zhu et al., 2014)]. The maintenance of several differentiated cell types is dependent on Nkx2.3 activity and loss of Nkx function alters cell identity [(Czompoly et al., 2011) (Targoff et al., 2013)]. In this study, we found that loss of Nkx2.3 activity shifts the transcriptomic profile from mucous acinar cells toward that of serous acinar cells. We conclude that Nkx2.3 regulates the expression of genes required for maintaining the mucous acinar cell identity in the SLG. The transcriptional profile of the SLG_{KO} is intermediate between that of the SLG_{WT} and the PG_{WT}, which suggests that Nkx2.3 acts in concert with other SLG-specific transcription factors to specify mucous cell identity.

The down-regulation of several gene categories associated with mucous cell identity, including membrane channels, enzymes involved in glycosylation pathways and secreted proteases, indicates that Nkx2.3 transcriptional activity is required to maintain expression levels of these genes. However, the up-regulation of several genes associated with serous acinar cells in the absence of Nkx2.3 suggests that Nkx2.3 acts to repress their expression. This was supported by our finding of canonical Nkx2.3 binding sites in intronic sequences of the *Cpeb3* and *Ptprk* genes, both of which are significantly up-regulated in the *Nkx2.3−/−* SLG (data not shown). As observed in other tissues of *Nkx2.3−/−* mice [(Kellermayer et al., 2014)], these results indicate that Nkx2.3 transcription factor fills both activation and repressive functions in SLG cells. We conclude that Nkx2.3 plays a role in directing mucous cell identity and in repressing serous cell identity.

Nkx2.3 expression is localized to the pharyngeal endoderm and presumptive oral ectoderm by E8.0 [(Pabst et al., 1997) (Biben et al., 2002)] and is subsequently detected in the gut mesenchyme, spleen, and endothelial cells throughout development and in adult mice [(Pabst et al., 1999) (Wang et al., 2000)]. In *Nkx2.3−/−* mice, the spleen is severely reduced in size and the small intestine is abnormally developed [(Pabst et al., 1999) (Wang et al., 2000) (Tarlinton et al., 2003) (Pabst et al., 2000; Vojkovics et al., 2018)]. These defects result in postnatal lethality in 30% of homozygous $Nkx2.3^{lacZ\Delta HD}$ mutants [(Wang et al., 2000) (Pabst et al., 1999)]. Our analysis of the SLGs in $Nkx2.3^{lacZ\Delta HD}$ mutants included embryonic (E18.5) and early postnatal (P0, P5) homozygotes, as well as mice that survived to adulthood.

Abnormal leukocyte homing and severe structural changes in the spleen trigger immune surveillance and inflammatory responses in *Nkx2.3−/−* mice [(Kellermayer et al., 2014)]. Furthermore, the Nkx2.3 transcription factor regulates several signaling pathways central to inflammation or immune response [(Yu et al., 2011)]. Our data revealed the up-regulation of many genes in the SLG_{KO} encoding secretory proteins that are expressed at low levels in the SLG_{WT} and PG_{WT}. Many of these genes were associated with immune or inflammatory processes, including a group of significantly up-regulated secretoglobins. The increased expression of Pip, a protein highly expressed in serous cells, is consistent with a shift in gene expression from mucous to a serous cell pattern in the absence of Nkx2.3. In addition, analysis of a *Pip−/−* mouse model revealed that Pip plays a critical role in adaptive immunity and regulates genes involved in host defense [(Blanchard et al., 2009; Li et al., 2015)]. We propose that dysregulation of this category of genes is due to the systemic activation of inflammatory responses in *Nkx2.3−/−* mice.

The *Mucin19 (Muc19)* gene, made up of 60 exons, is alternatively spliced to generate two distinct transcripts, which encode separate secretory products produced by SLG mucous acinar cells, Muc19 and the much lower molecular weight SmgC [(Culp et al., 2004) (Zinzen et al., 2004)]. Expression of the two proteins appears to undergo a switch as the SLG develops, leading to the suggestion that alternative splicing of SmgC and Muc19 mRNAs is linked to the differentiation of mucous acinar cells [(Das et al., 2009)]. SmgC expression is high during late embryonic development and at birth, but rapidly declines by P14 [(Das et al., 2009)]. In contrast, Muc19 transcripts and protein are low during embryogenesis and become increasingly abundant after birth [(Das et al., 2009) (Das et al., 2010)]. In the *Nkx2.3−/−* SLG, we observed dysregulation of SmgC and Muc19 proteins during early postnatal development and both transcripts were up-regulated in the SLG_{KO} of adults. Inspection of the RNA-Seq data revealed at least 8 genes associated with splicing activity that were differentially expressed in the SLG_{KO} (4 up- and 4 down-regulated; data not shown). Although we did not directly investigate splicing transcripts, the data suggest that the splicing switch from Smgc to Muc19 expression is disrupted in the *Nkx2.3−/−* SLG.

In summary, we report that loss of Nkx2.3 activity in the SLG shifts the gene expression profile, resulting in acinar cells expressing a transcriptome that is intermediate between mucous and serous cells. The data suggest that the Nkx2.3 transcription factor plays both activating and repressive roles in the developing SLG, leading to dysregulation of salivary gland-specific and systemic genes, as well as potential alterations in RNA splicing and

protein processing. Interest in salivary gland development is driven by the critical need to address the irreversible loss of secretory acinar cells in patients following radiation therapy for head and neck cancers. Serous acinar cells are acutely sensitive to radiation while mucous acinar cells are less affected [(Stephens et al., 1986)]. This study demonstrates that the Nkx2.3 transcription factor acts in specifying the mucous acinar cell type. In both zebrafish and mice, loss of Nkx gene function leads to reprogramming or transdifferentiation of the expressing cell types [(Kellermayer et al., 2014; Targoff et al., 2013)]. Understanding the role Nkx2.3 plays in controlling mucous cell identity offers a new tool for exploring whether acinar cells are malleable to reprogramming.

Materials and Methods

Chemicals were purchased from Sigma-Aldrich (St Louis, MO, USA) unless otherwise stated.

Animals

The *Nkx2.3*$^{lacZ\Delta HD}$ mouse model has been previously described [(Wang et al., 2000)] and has been cryopreserved and deposited at Jackson Laboratories (Strain# 416614, stored until 12/2024). *Nkx2.3*$^{lacZ\Delta HD}$ mice were maintained on a C57BL/6J background (Jackson Laboratories), and housed in pathogen-free, micro-isolator cages with free access to laboratory chow and water with a 12-hour light/dark cycle. *Nkx2.3*$^{lacZ\Delta HD}$ mice were mated to generate *Nkx2.3−/−* mice. Genotyping was done using three primers (Supplemental Table 4). Experiments were performed using male and female mice at 2 to 8 months old. Animal procedures were approved by the University of Rochester Committee for Animal Research (101362) and the Animal Care and Use Committee of the National Institute of Dental and Craniofacial Research, National Institutes of Health (ASP 16-802).

Tissue isolation

For RNA-Seq analysis, the SLGs were removed from 4 *Nkx2.3−/−* female mice (2 at 8 weeks, 2 at 32 weeks of age), immediately placed in liquid N2 and shipped on dry-ice overnight to Otogenetics Corporation (Atlanta, GA).

Body weights of wild type (WT), *Nkx2.3+/−* and surviving *Nkx2.3−/−* female mice were measured at P10, P14, P21 and adult (13.8 weeks). (n=4/group) The SLG were isolated individually, and the encapsulating membrane was removed. The SLG were then blotted and weighed immediately.

H&E and Alcian Blue staining of paraffin sections

SMG/SLG were isolated from *Nkx2.3−/−, Nkx2.3+/−*, and WT (*Nkx2.3+/+*) embryos at E18.5 or mice at P0, P5, and P21. Tissue was fixed overnight in 4% paraformaldehyde (PFA) at 4°C, then rinsed in 70% EtOH at 4°C. Tissue was processed using a Tissue-Tek VIP™ machine (Sakura Finetek USA, Inc.), embedded in paraffin, and cut into 5 μm sections. For H&E staining, sections were deparaffinized and stained with Gill's hematoxylin solution and eosin solution for 15 seconds. After washing with ethanol and

xylene, slides were mounted using Permount Mounting Medium (Fischer Scientific). Slides were left to dry in the fume hood overnight and imaged the next day.

For detection of polysaccharide staining in mucous acinar cells, paraffin-embedded sections were deparaffinized in xylene and dehydrated. The slides were incubated in Alcian blue (3% in Acetic acid, pH 2.5) for 3 minutes at room temperature. After washing with distilled water, the sections were counter stained with Nuclear Fast Red for 3 minutes and then rinsed and dehydrated in ethanol (70-95-100%) and in xylene. Stained sections were mounted with Permount (Fischer Scientific) and imaged.

Beta-galactosidase staining

SMG/SLG were isolated from *Nkx2.3−/−, Nkx2.3+/−*, and WT (*Nkx2.3+/+*) embryos at E18.5 or mice at P5 and P21. Tissue was fixed in 4% PFA for 30 minutes at 4°C. Samples were processed through sucrose gradients in PBS (5-10-15%, and then 1:1 mixture OCT:30% sucrose in PBS) at 4°C as described [(Aure et al., 2015)] and embedded in Tissue Tek OCT™ compound (Sakura Finetek USA, Inc.). Frozen sections were post-fixed in 0.2% PFA for 10 min on ice, rinsed twice with 1xPBS with 2mM $MgCl_2$, and 10 minutes with detergent buffer (0.1M phosphate buffer with 2 mM $MgCl_2$, 0.01% Na-deoxycholate, 0.02% IGEPAL, 5mM EGTA, pH 7.4). Sections were stained for beta-galactosidase overnight at 37°C in 0.1M phosphate buffer with 2mM $MgCl_2$, 0.01% Na-deoxycholate, 0.02% IGEPAL, 5mM potassium ferricyanide, 5mM potassium ferrocyanide and 1mg/ml X-GAL (ThermoFisher) in 0.1M phosphate buffer, pH 7.4. Sections were rinsed twice in 1xPBS with 2mM $MgCl_2$, counterstained with Nuclear Fast Red (Vector labs), dehydrated (in 70-95-100% ethanol- xylene) and coverslips were mounted using Permount (Fischer Scientific).

Immunohistochemistry

Paraffin sections were deparaffinized in xylene and dehydrated. Antigen retrieval was performed in Tris-EDTA, pH9.0, using a pressure cooker for 10 minutes. After cooling, 10% normal donkey serum in PBS and 1% BSA was used to block non-specific binding at room temperature for 1 hour. For fluorescent labeling, sections were incubated overnight at 4°C with polyclonal Goat anti-mouse SmgC antibody (LS-C154825, Life Science Bio) at 1:200 dilution; or with rabbit anti-rat mucin 19 antisera [(Das et al., 2010; Fallon et al., 2003; Man et al., 1995)] at 1:500 dilution in PBS with 1% BSA. After rinsing in PBS/0.1% Tween and PBS, slides were incubated for 1 hour at room temperature with secondary antibodies: donkey anti-goat Alexa Fluor Plus 594 (A-32758, Invitrogen) diluted 1:500, or donkey anti-rabbit Alexa Fluor Plus 594 (A-21207, Invitrogen) diluted 1:500 in PBS with 1% BSA. After 3 washes in PBS, slides were incubated with DAPI (1:1000 dilution in 0.1% PBSA; Molecular Probes) for 5 minutes, washed in PBS, and mounted with Immu-Mount (Thermo Fisher). Staining for each antibody was performed on 5 – 7 sections per sample; samples were collected from a minimum of four animals (males and females) for each genotype and at least three animals per sex per age group (E18.5, P0, P5, P21, adult over 20 weeks).

Imaging

Brightfield images were taken using an Olympus BX41 microscope with PANFL objectives 10x, 20x, 40x and an Olympus DP71 digital camera and DP Controller software. Fluorescent images were taken using an Olympus iX81 microscope and Hamamatsu CCD camera. Images were merged and processed using MetaMorph control software.

RNA preparation and next-generation sequencing

RNA-Seq was performed as described [(Gao et al., 2018)]. Briefly, total RNA was extracted using the RNeasy Micro Kit (Qiagen, Valencia, CA, catalog #74004). cDNA was generated from high quality total RNA using the SMARTer PCR cDNA Synthesis Kit with modified oligo(dT) primers (Clontech Laboratories, Inc., Mountain View, CA, catalog #634926), and adapters were removed by digestion with *Rsa*I. The resulting cDNA were fragmented using Bioruptor (Diagenode Inc., Denville, NJ) and Illumina libraries made from qualified fragmented cDNA using the SPRIworks HT Reagent Kit (Beckman Coulter, Inc., Indianapolis, IN, #B06938). The libraries were submitted for Illumina HiSeq2500 sequencing according to the standard operation with v1 or v2 chemistry, and 100-106 nucleotide paired end reads were generated and checked for data quality using FastQC (Babraham Institute, Cambridge, UK). Each library was sequenced at approximately 40 million reads.

Analysis and comparison of RNA-Seq data

The data were analyzed using the platform provided by DNAnexus (Mountain View, CA) and then: (1) mapped against the mouse mm10 reference genome with STAR 2.4.0j [(Dobin et al., 2013)], and the expression level of genes was quantified using htseq-count [(Anders et al., 2015)]. The resulting count data for *Nkx2.3*$^{-/-}$ SLG were then compared with wild type SLG and PG data (data from [(Gao et al., 2018)] using DESeq2 [(Love et al., 2014)] after batch correction with RUVseq [(Risso et al., 2014)]. A cutoff of $q<0.05$ was used for significance of differentially expressed genes. (2) measured for expression levels of genes and transcripts with Salmon [(Patro et al., 2017)] to obtain TPM (transcripts per million). TPM is a library size-normalized count of a transcript's abundance, and it was used for the dataset in the present study since it is robust for cross-project comparison with a sum of all the values within any sample to be 1 million. The principal component analysis (PCA) plots, heat maps, boxplots, and cluster dendrograms were created in RStudio using the TPM values. The heat maps were clustered by rows (genes). Box plots were created where the middle line represents the median and the box represents the middle 50% of data points. The Gene Ontology annotation was derived from the Gene Ontology Consortium database (http://geneontology.org), which was further supplemented with InterProScan output [(Jones et al., 2014)] and the enrichment test was performed using FUNC packages [(Prufer et al., 2007)].

Quantitative RT-PCR

RNA was isolated from SLG and PG, and cDNA samples were synthesized using the BioRad iScript cDNA synthesis kit (BioRad 1708890). qPCR was carried out in 96-well plates using BioRad SSO Advance SYBR mix (BioRad 1725270) with the standard SSO

Advanced protocol (40 cycles) in a BioRad CfX96 Real Time Thermocycler. To compare transcript levels between the SLG and PG, we tested 8 reference genes to determine their expression levels in the two major salivary glands [(Svingen et al., 2015)]. All primers were validated using an annealing temperature of 60°C. LE32 and B2M were chosen as reference genes based on similar Ct values in SLG and PG. Relative quantities were calculated by means of real-time PCR using the $2^{-\Delta\Delta Ct}$ comparative method. Primer sequences are listed in Supplemental Table 4.

Ex vivo perfusion of salivary glands

Male and female mice were used for *ex vivo* saliva collection. Male (n=12) and female (n=6) WT and male (n=10) and female (n=5) Nkx2.3−/− mice were weighed and anesthetized by intraperitoneal (i.p.) injection of chloral hydrate (400mg/kg body weight). All divisions of the carotid artery were ligated, except for the submandibular and sublingual arteries. The glands were then transferred to a perfusion chamber in which the common carotid artery was cannulated (31G) and perfused with experimental solutions at 37°C. Gland-specific saliva was collected separately from the SLG and SMG by inserting the distal ends of their ducts into individual calibrated glass capillary tubes (Sigma-Aldrich). Secretion was stimulated using cholinergic (carbachol, 0.3μM) and β-adrenergic (isoproterenol, 1μM) agonists. The flow rate and total amount of collected saliva were measured by recording the saliva's progression through the capillary tube every 5 minutes. The saliva collected within the capillary tube after 30 min stimulation was stored at −86°C. Bar graphs were generated using the mean and standard error. Significance was determined using Student's *t* test or ANOVA and Bonferroni's post hoc test, with $p<0.05$ considered to be statistically significant. Separate bar graphs of saliva collected from male and female *Nkx2.3+/+* and *Nkx2.3−/−* mice showed no significant differences. For this reason, saliva volumes were standardized to μl/minute per 100mg of gland weight, and data from males and females was combined in the graphs.

Proteomics of *ex vivo* sublingual salivary gland saliva

Saliva was collected as described from the left and/or right SLG of male and female *Nkx2.3+/+* and *Nkx2.3−/−* mice. Due to the low volume of saliva collected, samples were pooled and each sample was split into 5 replicates and analyzed by LC-MS/MS as previously described [(Stopka et al., 2016)]. Briefly, protein was precipitated overnight by trichloroacetic acid (TCA) and pellet dissolved and denatured with 6 M urea, reduced with 200 mM dithiothreitol for 60 min at room temperature followed by alkylation with 200 mM iodoacetamide at room temperature in the dark for 60 min. The urea was diluted with ammonium bicarbonate prior to digestion by trypsin (Promega) overnight at 37°C with gentle shaking at a protein-to-trypsin ratio of 30:1(w/w). Peptides were desalted using Oasis HLB-1 (1 mg) reversed phase cartridge (Waters) and vacuum concentrated to dryness. Tryptic peptides were labeled by iTRAQ for quantification as previously described [(Hardt et al., 2005)]. Five micrograms of tryptic peptide iTRAQ mixtures were loaded onto Zorbax C_{18} trap column (Agilent Tech.) for 8.3 min at a flow rate of 6.0 μL/min for further desalting. The peptides were then separated on a 10 cm Picofrit Biobasic C_{18} analytical column (New Objective) using an on-line Eksigent (Dublin, CA) nano-LC ultra HPLC system. The peptides were eluted using a 120 min acetonitrile gradient (5–35 %) at flow

rate of 250 nL/min. Peptides were ionized using electrospray ionization (ESI) in positive ion mode and detected on a LTQ-Orbitrap Velos (Thermo Fisher Scientific). Precursor ions were selected for MS/MS using a data-dependent method in which the top 6 most intense ions from the MS1 precursor scan were selected. All precursor ions were measured in the Orbitrap with the resolution set at 30,000 (m/z 400). Precursor ions were fragmented by collision-induced dissociation (CID) with normalized collision energy of 35%, and all fragment ions were measured in the LTQ. The targeted LC-MS/MS runs were 1 h, while the discovery runs were 2 h. All LC-MS/MS data were searched using the MASCOT algorithm within Proteome Discoverer 1.3 (Thermo Electron Corp) against human Swissprot protein database (Version Sprot_101911) to obtain peptide and protein identifications. For all searches, trypsin was specified as the enzyme for protein cleavage allowing up to 2 missed cleavages. Oxidation (M) and carbamidomethylation (C) were set as dynamic and fixed modifications. Mass tolerance of 20 ppm and 0.8 Da were set for precursor and fragment ions, respectively.

The data set containing up- and down-regulated proteins (≤0.5) were analyzed by Ingenuity Pathway Analysis version 9.0 (Ingenuity® Systems, www.ingenuity.com). Statistically significant protein identification by IPA is based on mapping input proteins with a continuously curated database of published literature to a range of function, cellular location, canonical pathways and disease interrelationships. The association between proteins in the data-set and canonical pathways in the Ingenuity Pathways Knowledge Base was measured as a ratio of the number of molecules from the data that maps to a pathway divided by the total number of molecules that map to the canonical pathway. A right-tailed Fisher's Exact Test was used to calculate the *p*-value of the probability that the association between each protein in the dataset and the canonical pathway is random.

Supplementary Material

Refer to Web version on PubMed Central for supplementary material.

Acknowledgements

The *Nkx2-3*$^{lacZ\Delta HD}$ mouse model was a generous donation from Dr. Lily Mirels to CEO. The authors wish to thank Dr. Art Hand (University of Connecticut) for critical discussions during the development of the study, Dr. Marit Aure (NIDCR) for critical assistance with histological and immunofluorescent staining, and Dr. Murat Sincan (University of South Dakota) for invaluable assistance in the saliva proteomic experiment. We thank Yasna Jaramillo and Eri Maruyama for excellent technical assistance. This study was supported by the Intramural Research Program of the National Institute of Dental and Craniofacial Research, National Institutes of Health (JEM, ZIA DE000738; Veterinary Research Core, 1-ZIG-DE000740) and NIDCR R01 DE008921 (CEO).

References

Anders S, Pyl PT, Huber W, 2015. HTSeq--a Python framework to work with high-throughput sequencing data. Bioinformatics 31, 166–169. [PubMed: 25260700]

Athwal HK, Murphy G 3rd, Tibbs E, Cornett A, Hill E, Yeoh K, Berenstein E, Hoffman MP, Lombaert IMA, 2019. Sox10 Regulates Plasticity of Epithelial Progenitors toward Secretory Units of Exocrine Glands. Stem Cell Reports 12, 366–380. [PubMed: 30713042]

Aure MH, Konieczny SF, Ovitt CE, 2015. Salivary gland homeostasis is maintained through acinar cell self-duplication. Dev Cell 33, 231–237. [PubMed: 25843887]

Biben C, Wang CC, Harvey RP, 2002. NK-2 class homeobox genes and pharyngeal/oral patterning: Nkx2-3 is required for salivary gland and tooth morphogenesis. Int J Dev Biol 46, 415–422. [PubMed: 12141427]

Blanchard A, Nistor A, Castaneda FE, Martin D, Hicks GG, Amara F, Shiu RP, Myal Y, 2009. Generation and initial characterization of the prolactin-inducible protein (PIP) null mouse: accompanying global changes in gene expression in the submandibular gland. Can J Physiol Pharmacol 87, 859–872. [PubMed: 20052012]

Chatzeli L, Gaete M, Tucker AS, 2017. Fgf10 and Sox9 are essential for the establishment of distal progenitor cells during mouse salivary gland development. Development 144, 2294–2305. [PubMed: 28506998]

Culp DJ, Latchney LR, Fallon MA, Denny PA, Denny PC, Couwenhoven RI, Chuang S, 2004. The gene encoding mouse Muc19: cDNA, genomic organization and relationship to Smgc. Physiol Genomics 19, 303–318. [PubMed: 15340121]

Czompoly T, Labadi A, Kellermayer Z, Olasz K, Arnold HH, Balogh P, 2011. Transcription factor Nkx2-3 controls the vascular identity and lymphocyte homing in the spleen. J Immunol 186, 6981–6989. [PubMed: 21593383]

Das B, Cash MN, Hand AR, Shivazad A, Culp DJ, 2009. Expression of Muc19/Smgc gene products during murine sublingual gland development: cytodifferentiation and maturation of salivary mucous cells. J Histochem Cytochem 57, 383–396. [PubMed: 19110483]

Das B, Cash MN, Hand AR, Shivazad A, Grieshaber SS, Robinson B, Culp DJ, 2010. Tissue distibution of murine Muc19/smgc gene products. J Histochem Cytochem 58, 141–156. [PubMed: 19826070]

Denny PC, Ball WD, Redman RS, 1997. Salivary glands: a paradigm for diversity of gland development. Crit Rev Oral Biol Med 8, 51–75. [PubMed: 9063625]

Desai S, Loomis Z, Pugh-Bernard A, Schrunk J, Doyle MJ, Minic A, McCoy E, Sussel L, 2008. Nkx2.2 regulates cell fate choice in the enteroendocrine cell lineages of the intestine. Dev Biol 313, 58–66. [PubMed: 18022152]

Dobin A, Davis CA, Schlesinger F, Drenkow J, Zaleski C, Jha S, Batut P, Chaisson M, Gingeras TR, 2013. STAR: ultrafast universal RNA-seq aligner. Bioinformatics 29, 15–21. [PubMed: 23104886]

Fallon MA, Latchney LR, Hand AR, Johar A, Denny PA, Georgel PT, Denny PC, Culp DJ, 2003. The sld mutation is specific for sublingual salivary mucous cells and disrupts apomucin gene expression. Physiol Genomics 14, 95–106. [PubMed: 12847143]

Gao X, Oei MS, Ovitt CE, Sincan M, Melvin JE, 2018. Transcriptional profiling reveals gland-specific differential expression in the three major salivary glands of the adult mouse. Physiol Genomics 50, 263–271. [PubMed: 29373073]

Hardt M, Witkowska HE, Webb S, Thomas LR, Dixon SE, Hall SC, Fisher SJ, 2005. Assessing the effects of diurnal variation on the composition of human parotid saliva: quantitative analysis of native peptides using iTRAQ reagents. Anal Chem 77, 4947–4954. [PubMed: 16053308]

Harvey RP, 1996. NK-2 homeobox genes and heart development. Dev Biol 178, 203–216. [PubMed: 8812123]

Jones P, Binns D, Chang HY, Fraser M, Li W, McAnulla C, McWilliam H, Maslen J, Mitchell A, Nuka G, Pesseat S, Quinn AF, Sangrador-Vegas A, Scheremetjew M, Yong SY, Lopez R, Hunter S, 2014. InterProScan 5: genome-scale protein function classification. Bioinformatics 30, 1236–1240. [PubMed: 24451626]

Kellermayer Z, Mihalj M, Labadi A, Czompoly T, Lee M, O'Hara E, Butcher EC, Berta G, Balogh A, Arnold HH, Balogh P, 2014. Absence of Nkx2-3 homeodomain transcription factor reprograms the endothelial addressin preference for lymphocyte homing in Peyer's patches. J Immunol 193, 5284–5293. [PubMed: 25320278]

Kim Y, Nirenberg M, 1989. Drosophila NK-homeobox genes. Proc Natl Acad Sci U S A 86, 7716–7720. [PubMed: 2573058]

Li B, Qing T, Zhu J, Wen Z, Yu Y, Fukumura R, Zheng Y, Gondo Y, Shi L, 2017. A Comprehensive Mouse Transcriptomic BodyMap across 17 Tissues by RNA-seq. Sci Rep 7, 4200. [PubMed: 28646208]

Li J, Liu D, Mou Z, Ihedioha OC, Blanchard A, Jia P, Myal Y, Uzonna JE, 2015. Deficiency of prolactin-inducible protein leads to impaired Th1 immune response and susceptibility to Leishmania major in mice. Eur J Immunol 45, 1082–1091. [PubMed: 25594453]

Love MI, Huber W, Anders S, 2014. Moderated estimation of fold change and dispersion for RNA-seq data with DESeq2. Genome Biol 15, 550. [PubMed: 25516281]

Man YG, Ball WD, Culp DJ, Hand AR, Moreira JE, 1995. Persistence of a perinatal cellular phenotype in submandibular glands of adult rat. J Histochem Cytochem 43, 1203–1215. [PubMed: 8537636]

Miletich I, 2010. Introduction to salivary glands: structure, function and embryonic development. Front Oral Biol 14, 1–20. [PubMed: 20428008]

Mootz M, Jakwerth CA, Schmidt-Weber CB, Zissler UM, 2022. Secretoglobins in the big picture of immunoregulation in airway diseases. Allergy 77, 767–777. [PubMed: 34343347]

Pabst O, Forster R, Lipp M, Engel H, Arnold HH, 2000. NKX2.3 is required for MAdCAM-1 expression and homing of lymphocytes in spleen and mucosa-associated lymphoid tissue. EMBO J 19, 2015–2023. [PubMed: 10790368]

Pabst O, Schneider A, Brand T, Arnold HH, 1997. The mouse Nkx2-3 homeodomain gene is expressed in gut mesenchyme during pre- and postnatal mouse development. Dev Dyn 209, 29–35. [PubMed: 9142493]

Pabst O, Zweigerdt R, Arnold HH, 1999. Targeted disruption of the homeobox transcription factor Nkx2-3 in mice results in postnatal lethality and abnormal development of small intestine and spleen. Development 126, 2215–2225. [PubMed: 10207146]

Patel VN, Hoffman MP, 2014. Salivary gland development: a template for regeneration. Semin Cell Dev Biol 25–26, 52–60.

Patro R, Duggal G, Love MI, Irizarry RA, Kingsford C, 2017. Salmon provides fast and bias-aware quantification of transcript expression. Nat Methods 14, 417–419. [PubMed: 28263959]

Prufer K, Muetzel B, Do HH, Weiss G, Khaitovich P, Rahm E, Paabo S, Lachmann M, Enard W, 2007. FUNC: a package for detecting significant associations between gene sets and ontological annotations. BMC Bioinformatics 8, 41. [PubMed: 17284313]

Redman RS, Ball WD, 1978. Cytodifferentiation of secretory cells in the sublingual gland of the prenatal rat: a histological, histochemical and ultrastructural study. Am J Anat 153, 367–389. [PubMed: 707321]

Risso D, Ngai J, Speed TP, Dudoit S, 2014. Normalization of RNA-seq data using factor analysis of control genes or samples. Nat Biotechnol 32, 896–902. [PubMed: 25150836]

Rothova M, Thompson H, Lickert H, Tucker AS, 2012. Lineage tracing of the endoderm during oral development. Dev Dyn 241, 1183–1191. [PubMed: 22581563]

Saitou M, Gaylord EA, Xu E, May AJ, Neznanova L, Nathan S, Grawe A, Chang J, Ryan W, Ruhl S, Knox SM, Gokcumen O, 2020. Functional Specialization of Human Salivary Glands and Origins of Proteins Intrinsic to Human Saliva. Cell Rep 33, 108402. [PubMed: 33207190]

Stanfel MN, Moses KA, Schwartz RJ, Zimmer WE, 2005. Regulation of organ development by the NKX-homeodomain factors: an NKX code. Cell Mol Biol (Noisy-le-grand) Suppl 51, OL785–799.

Stephens LC, Ang KK, Schultheiss TE, King GK, Brock WA, Peters LJ, 1986. Target cell and mode of radiation injury in rhesus salivary glands. Radiother Oncol 7, 165–174. [PubMed: 3786822]

Stopka P, Kuntova B, Klempt P, Havrdova L, Cerna M, Stopkova R, 2016. On the saliva proteome of the Eastern European house mouse (Mus musculus musculus) focusing on sexual signalling and immunity. Sci Rep 6, 32481. [PubMed: 27577013]

Sussel L, Kalamaras J, Hartigan-O'Connor DJ, Meneses JJ, Pedersen RA, Rubenstein JL, German MS, 1998. Mice lacking the homeodomain transcription factor Nkx2.2 have diabetes due to arrested differentiation of pancreatic beta cells. Development 125, 2213–2221. [PubMed: 9584121]

Svingen T, Letting H, Hadrup N, Hass U, Vinggaard AM, 2015. Selection of reference genes for quantitative RT-PCR (RT-qPCR) analysis of rat tissues under physiological and toxicological conditions. PeerJ 3, e855. [PubMed: 25825680]

Targoff KL, Colombo S, George V, Schell T, Kim SH, Solnica-Krezel L, Yelon D, 2013. Nkx genes are essential for maintenance of ventricular identity. Development 140, 4203–4213. [PubMed: 24026123]

Tarlinton D, Light A, Metcalf D, Harvey RP, Robb L, 2003. Architectural defects in the spleens of Nkx2-3-deficient mice are intrinsic and associated with defects in both B cell maturation and T cell-dependent immune responses. J Immunol 170, 4002–4010. [PubMed: 12682228]

Urbaniak A, Jablonska K, Podhorska-Okolow M, Ugorski M, Dziegiel P, 2018. Prolactin-induced protein (PIP)-characterization and role in breast cancer progression. Am J Cancer Res 8, 2150–2164. [PubMed: 30555735]

Vojkovics D, Kellermayer Z, Kajtar B, Roncador G, Vincze A, Balogh P, 2018. Nkx2-3-A Slippery Slope From Development Through Inflammation Toward Hematopoietic Malignancies. Biomark Insights 13, 1177271918757480. [PubMed: 29449776]

Wang CC, Biben C, Robb L, Nassir F, Barnett L, Davidson NO, Koentgen F, Tarlinton D, Harvey RP, 2000. Homeodomain factor Nkx2-3 controls regional expression of leukocyte homing coreceptor MAdCAM-1 in specialized endothelial cells of the viscera. Dev Biol 224, 152–167. [PubMed: 10926756]

Wang YC, Gallego-Arteche E, Iezza G, Yuan X, Matli MR, Choo SP, Zuraek MB, Gogia R, Lynn FC, German MS, Bergsland EK, Donner DB, Warren RS, Nakakura EK, 2009. Homeodomain transcription factor NKX2.2 functions in immature cells to control enteroendocrine differentiation and is expressed in gastrointestinal neuroendocrine tumors. Endocr Relat Cancer 16, 267–279. [PubMed: 18987169]

Xu XM, Chen Y, Chen J, Yang S, Gao F, Underhill CB, Creswell K, Zhang L, 2003. A peptide with three hyaluronan binding motifs inhibits tumor growth and induces apoptosis. Cancer Res 63, 5685–5690. [PubMed: 14522884]

Yoshida S, Ohbo K, Takakura A, Takebayashi H, Okada T, Abe K, Nabeshima Y, 2001. Sgn1, a basic helix-loop-helix transcription factor delineates the salivary gland duct cell lineage in mice. Dev Biol 240, 517–530. [PubMed: 11784080]

Yu W, Hegarty JP, Berg A, Chen X, West G, Kelly AA, Wang Y, Poritz LS, Koltun WA, Lin Z, 2011. NKX2-3 transcriptional regulation of endothelin-1 and VEGF signaling in human intestinal microvascular endothelial cells. PLoS One 6, e20454. [PubMed: 21637825]

Zhu Q, Zhao X, Zheng K, Li H, Huang H, Zhang Z, Mastracci T, Wegner M, Chen Y, Sussel L, Qiu M, 2014. Genetic evidence that Nkx2.2 and Pdgfra are major determinants of the timing of oligodendrocyte differentiation in the developing CNS. Development 141, 548–555. [PubMed: 24449836]

Zinzen KM, Hand AR, Yankova M, Ball WD, Mirels L, 2004. Molecular cloning and characterization of the neonatal rat and mouse submandibular gland protein SMGC. Gene 334, 23–33. [PubMed: 15256252]

Highlights

- Nkx2.3 transcription factor is a key regulator specifying mucous acinar cell identity.
- Nkx2.3 KO SLG transcriptome is intermediate between mucous and serous acinar cells.
- The Nkx2.3 transcription factor has both activating and repressive activities.

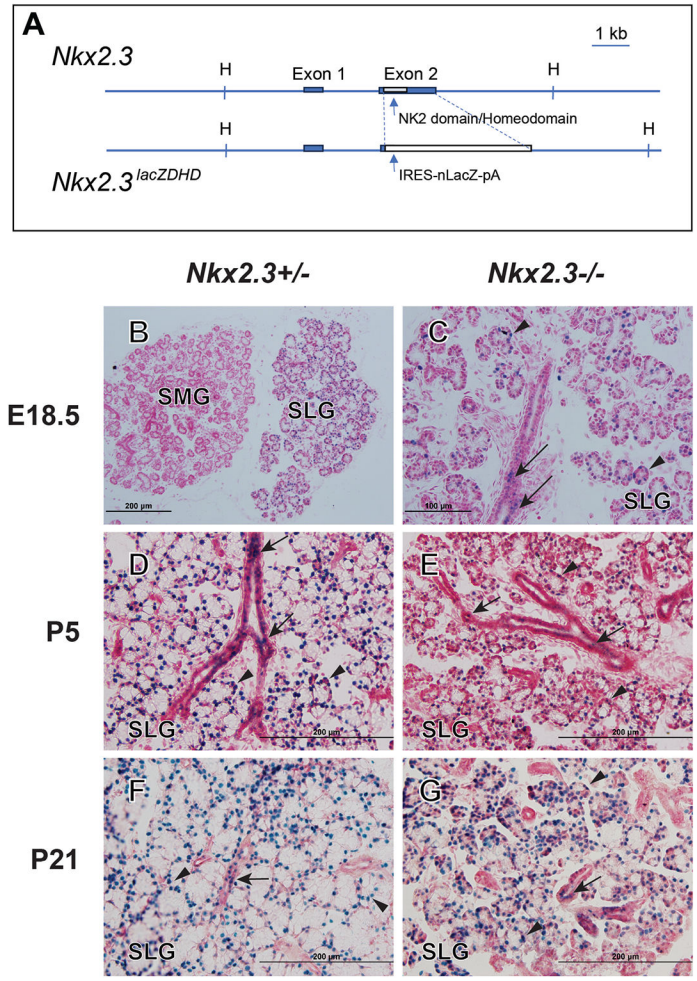

Figure 1. nLacZ expression driven by the *Nkx2.3* allele in *Nkx2.3*+/− and *Nkx2.3*−/− SLG.

A. Schematic diagram of wild-type *Nkx2.3* allele encoded by two exons (top), and the *Nkx2.3*$^{lacZ\Delta HD}$ allele (bottom), in which the homeodomain and conserved NK2-specific domains encoded in exon 2 of the *Nkx2.3* gene were replaced with an internal ribosome entry site (IRES) linked to a nuclear beta-galactosidase (nLacZ) gene expression cassette and polyadenylation (pA) site. (Modified from [(Wang et al., 2000)]). **B-G** Beta-galactosidase (blue) and H&E (red) staining of frozen sections from *Nkx2.3+/−* and *Nkx2.3−/−* SLG isolated at (**B,C**) E18.5, (**D,E**) P5 and (**F,G**) P21. **B**, nLacZ expression (blue) driven from the Nkx2.3 promoter is detected only in the SLG, but not in the SMG. (10x) **C**, H&E staining (red) shows that Nkx2.3-driven expression of nLacZ (blue) is present in both acinar (arrowheads) and duct cells (arrows) in the *Nkx2.3*$^{lacZ\Delta HD}$ SLG. (20x) **C,E,G**, In mice with 2 copies of the *Nkx2.3*$^{lacZ\Delta HD}$ allele (*Nkx2.3−/−*), the SLG shows disrupted morphology and disorganized mucous acinar cells. (20X) Scale bars= 200 μm (**B, D-G**), 100 μm (**C**)

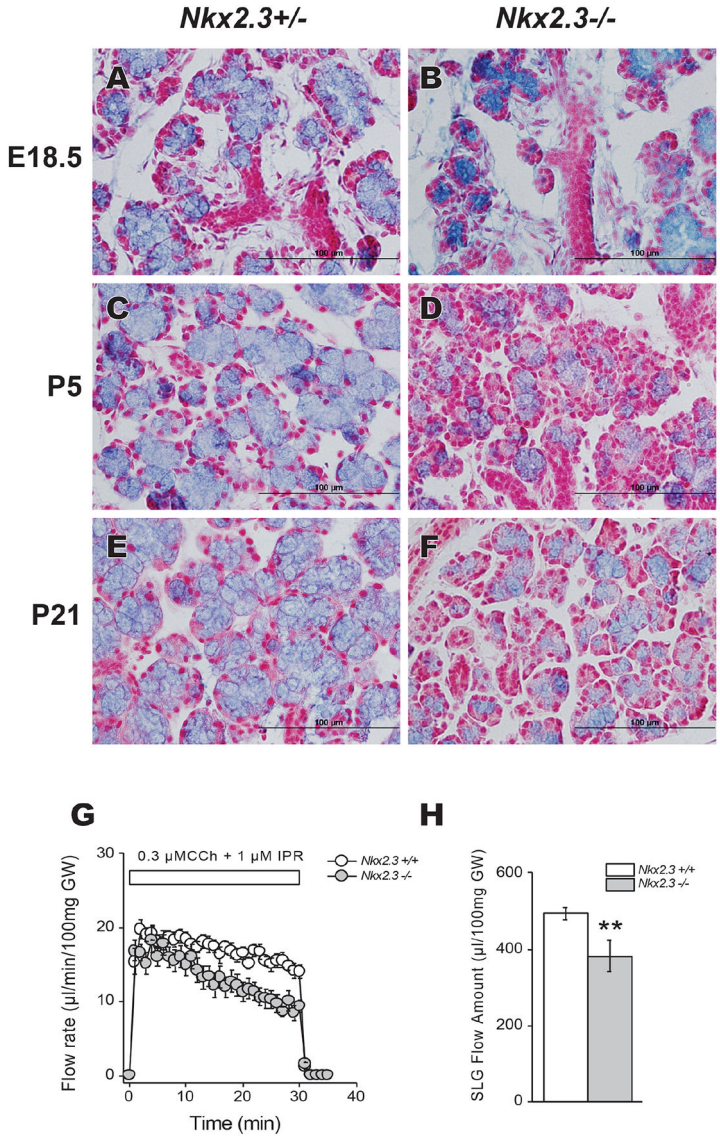

Figure 2. Comparison of morphology and saliva secretion from *Nkx2.3*+/− and *Nkx2.3*−/− SLG.

A-F, Alcian blue stains acidic mucins produced by mucous acinar cells in sublingual gland (SLG). Alcian blue (blue) and H&E (red) staining on sections of SLG from *Nkx2.3* +/− (**A,C,E**) and *Nkx2.3* −/− (**B,D,F**) mice isolated at (**A,B**) embryonic day 18.5 (E18.5), (**C,D**) postnatal day 5 (P5), and (**E,F**) postnatal day 21 (P21). All photos 40x. Scale bars = 100µm

G,H, Ex vivo saliva flow rate from SLG of *Nkx2.3+/+* (n=18) and *Nkx2.3−/−* (n=15) mice after stimulation with 0.3µm carbachol and 1µm isoproterenol. Saliva flow (µl/minute) was standardized to 100mg gland weight. Due to no significant differences between males and females, data is combined in the graphs. **p=0.006

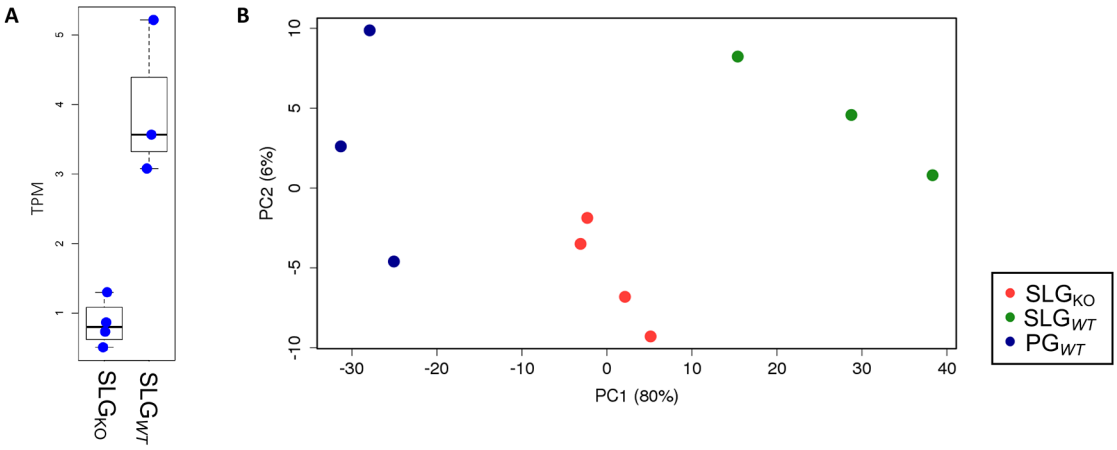

Figure 3. *Nkx2.3*−/− SLG transcriptome is intermediate between mucous and serous acinar cells.

A. Expression of *Nkx2.3* transcripts in *NKx2.3* +/+ (SLG_{WT}) and *NKx2.3* −/− (SLG_{KO}) SLG measured in transcripts per million (TPM). Expression of *Nkx2.3* transcripts in SLG_{KO} was 5-fold lower (0.85 TPM) than in SLG_{WT} (3.95 TPM). B. Principal component analysis (PCA) plot shows transcriptional profiles obtained by RNA-Seq of female *NKx2.3* −/− (SLG_{KO}, red symbols, n=4), in comparison to female mouse parotid (PG_{WT}, blue symbols, n=3), and female wild type sublingual (SLG_{WT}, green symbols, n=3). The corresponding data were submitted with accession number GSE168253 to the NCBI Gene Expression Omnibus database.

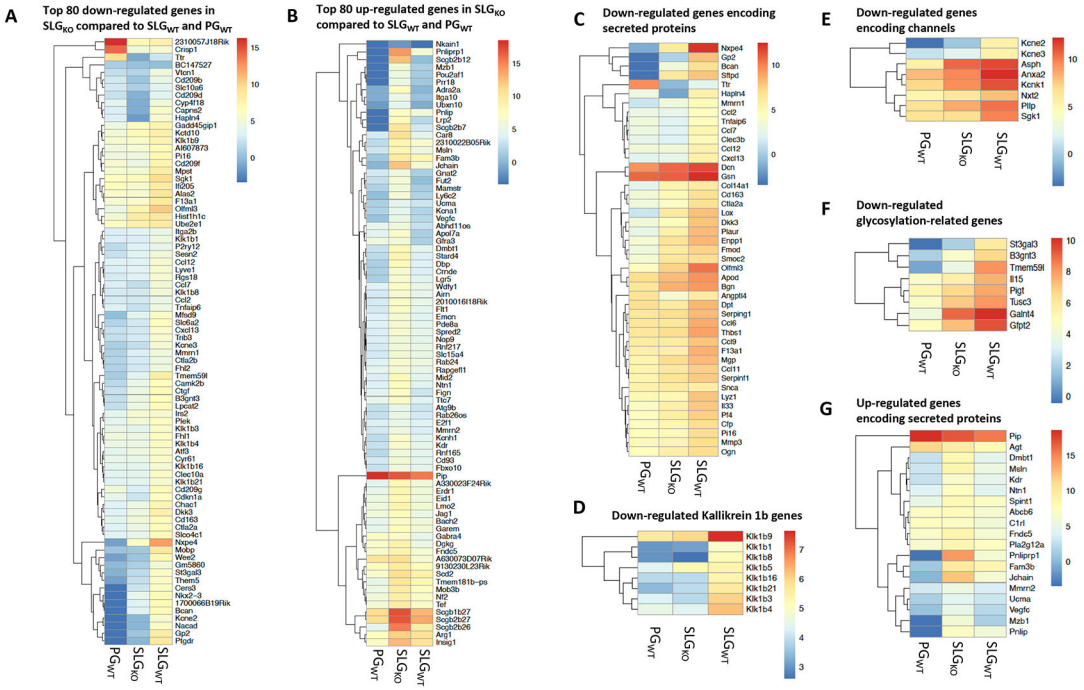

Figure 4. Expression profiles of up- and down-regulated genes in SLG$_{KO}$ compared to SLG$_{WT}$ and PG$_{WT}$.

Heat maps showing the gene expression level (Log2 (length scaled TPM) in SLG$_{KO}$, SLG$_{WT}$ and PG$_{WT}$ (data from [(Gao et al., 2018)]) of **(A)** the top 80 down-regulated genes (total number of significantly down-regulated DE genes = 262) and **(B)** the top 80 up-regulated genes (total number of significantly up-regulated DE genes = 234). **C-G** Heat maps of significantly DE genes in SLG$_{KO}$ compared with SLG$_{WT}$ and with PG$_{WT}$ (data from Gao et al. 2018), separated by protein function. **C.** Group of 48 down-regulated genes encoding secretory proteins in SLG$_{KO}$ compared to SLG$_{WT}$ and PG$_{WT}$. **D.** Down-regulated genes encoding Kallikrein1b protein family members in SLG$_{KO}$ compared to SLG$_{WT}$ and PG$_{WT}$. **E.** Expression levels of genes encoding membrane channels in SLG$_{KO}$ compared to SLG$_{WT}$ and PG$_{WT}$. **F.** Expression levels of several glycosylation-related genes are down-regulated in SLG$_{KO}$ compared to SLG$_{WT}$. **G.** Up-regulated genes encoding secreted proteins are expressed at higher level in SLG$_{KO}$ compared to SLG$_{WT}$ and PG$_{WT}$.

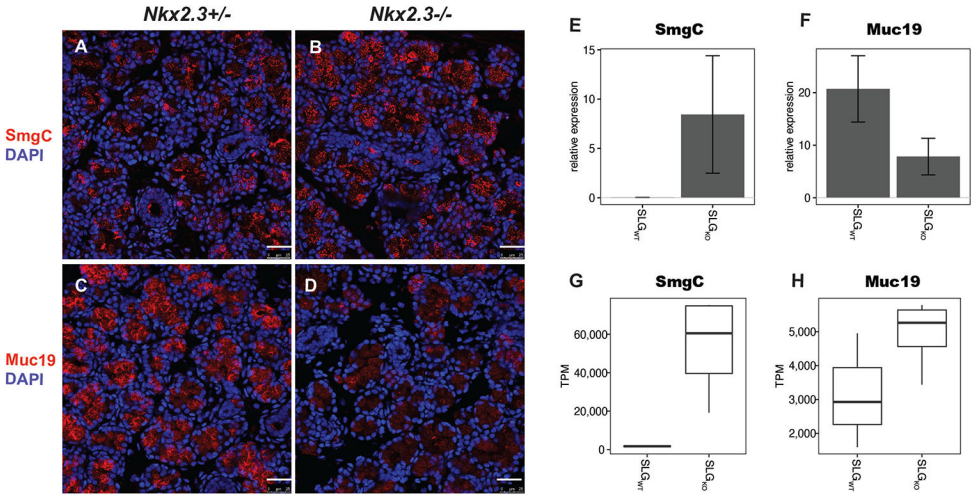

Figure 5. Expression of SmgC and Muc19 mRNA and proteins is disrupted in *Nkx2.3−/−* SLG.

A,B. Paraffin sections of *Nkx2.3+/−* and *Nkx2.3−/−* SLG isolated at P0 stained with antibody to SmgC. **C,D.** Paraffin sections of *Nkx2.3+/−* and *Nkx2.3−/−* SLG isolated at P0 stained with antisera to Muc19. Scale bars= 25μm **E,F.** Quantitative PCR using mRNA from *Nkx2.3+/−* and *Nkx2.3−/−* SLG at P21 for **(E)** SmgC and **(F)** Muc19. LE32 and B2M were used as reference genes. (N= 2 males, 2 females, 3-4 replicate experiments per sample; p= n.s.) Note that the changes detected by q-PCR (E,F) are not statistically significant. **G,H.** Box plots showing transcript levels of **(G)** SmgC and **(H)** Muc19 detected in RNA-Seq analysis of *Nkx2.3+/+* (SLG_{WT}) and *Nkx2.3−/−* (SLG_{KO}) adult mice at 33 weeks of age. (p=n.s.)